State-of-Charge Estimation to Improve Energy Conservation and Extend Battery Life of Wireless Sensor Network Nodes

Vanessa Quintero, Claudio Estevez, Marcos Orchard

Department of Electrical Engineering
Universidad de Chile
Santiago, Chile 8370451
Email: {vquintero, cestevez, morchard}@ing.uchile.cl

***Abstract*—Wireless sensor networks are pervasive systems that continuously demonstrate increase in growth by branching into diverse applications. The state of charge is an indicator that conveys the amount of energy available in the battery, information that contributes to better decision-making and energy-efficient protocols by creating smart cross-layer designs. WSN research trends portray the importance of energy-efficient systems by prioritizing energy efficiency over other arguably equally important aspects as throughput, channel utilization, latency, etc. This demonstrates the impact of improving the energy conservation techniques and extending the battery life of the sensor nodes. By using Bayesian inference, more specifically particle filtering, it is shown that the state of charge can be accurately estimated within the linear region of the voltage-SOC curve. Battery discharge experiments are compared to simulations of the voltage-SOC evolution behavior using a state-space representation model, which showed good agreement between the results. The SOC estimation obtained by the particle filter yields essential information that can, and should, be incorporated into MAC protocols.**

I. Introduction

Wireless sensor networks (WSNs) are widely used in a vast amount of applications and its use will continue to increase. Some examples that aid the portrayal of growth in the use of wireless sensing devices is observed in monitoring systems for healthcare [1] and environmental phenomena [2] [3]. Despite the advances and improvements exhibited by WSN technology for energy conservation, this remains a critical point that directly influences the performance and lifetime of the network. Several solutions have been proposed to improve the energy conservation in WSN, some of these have focused on the MAC protocols [4] [5], as they directly affect the operating modes of the sensor nodes allowing an improved power management, therefore reducing the energy consumption and thus prolonging the life of the network. A significant difference between traditional (oriented to cabled communications) MAC protocols and those designed for WSN is the emphasis given to the power management of the network, thus characteristics such as scalability, adaptability, fairness, channel utilization, performance, and minimizing latency often become a secondary priority in the pursue of achieving greater energy efficiency in these networks [6] [7].

In [8] the lifetime of the network is defined as the lapse of time between the start of operation of the sensors and the failure of one or more sensors causing the network to become inoperative. Various works are developed to estimate the lifetime of the network, regardless of whether they take in consideration the overall characteristics of the network or the individual batteries of each sensor [8] [9]. Having tools to estimate the lifetime of the network facilitates making timely decisions regarding its operation, leading to the development of autonomous and self-sustaining networks. As indicated above the estimated lifetime of the network can be made through the incorporation of information from the battery, for instance, the amount of energy available, commonly denoted as the state of charge (SOC), the temperature associated with charging and discharging the battery, the battery cell degradation, and other [10]. The SOC is a widely used indicator in applications where the amount of energy available in the battery can affect the proper operation of the device [10]. Due to the physical behavior exhibited by the batteries, the SOC cannot be measured directly. As a corollary, this induces the search for estimation methods capable of incorporating information from measurable variables such as the discharge current, voltage, and temperature [11]. In [12] authors indicate that the non-linear characteristics of the battery must be considered in the lifetime estimation as well as find a technique which incorporates aspects such as temperature and battery age that affect the node lifetime. The work in [12] summarizes the different methods used to estimate the capacity of the battery (electrochemical, voltage testing, and electromotive force) and the techniques used for the lifetime estimation in WSN based on voltage drop rate, quoted capacity and current consumption, quoted capacity, and energy consumption. Another example is presented in [13] where authors propose to determine the SOC through the open circuit voltage (OCV) measurement. The OCV voltage can be estimated by the power supply voltage of the sensor node using the Analog to Digital Converter (ADC)

present in the microcontroller of the sensor.

Over the last several years different methods have been used to estimate the SOC, such as the Ampere-hour meter [14], Open Circuit Voltage (OCV) measurement [15], Electrochemical Impedance Spectroscopy (EIS) [16] and methods based on battery modeling [10] [17] [18]. The methods based on the modeling of the battery allows to estimate the SOC in real-time and for the implementation of these methods it is necessary to characterize the battery using a model that can be electrochemical (physical), stochastic, or empirical [19] [20]. Among the methods based on battery modeling is the Bayesian inference, which includes techniques such as Kalman Filter (KF), Extended Kalman Filter (EKF) [21], and Particle Filter (PF) [22]. These Bayesian-filtering tools require a predicting step in which a state-space representation model allows us to estimate the SOC and to have an update layer where the observations are taken into consideration to further improve the accuracy of the estimation [23] [24].

This work presents a PF technique to estimate the SOC. PF is used here because it is a method that is able to estimate the battery charge in real-time and this facilitates the relevant information acquisition that may be considered by the MAC protocols for management control of the operating modes of the sensor. Moreover the SOC estimation based on PF allows to consider the non-lineal behavior of the battery, aspects that in WSN has been oversimplified by working with linear battery models [25].

II. Particle Filter

A PF is a sequential Monte Carlo method whose main idea is to represent the probability density function (pdf) through a set of random samples with associated weights [22] [26]. The PF consider to obtain samples from a target state probability distribution $\pi_k(x_{0:k})$ and it is oriented to generate a set of $N \gg 1$ particles with weights described by $\left\{w_k^{(i)}, x_{0:k}^{(i)} i=1...N\right.$, $w_k^{(i)} > 0, \forall k \geq 1$, such that:

$$\sum_{i=1}^{N} w_k^{(i)} \phi_k(x_{0:k}^{(i)}) \xrightarrow[N\to\infty]{} \int \phi_k(x_{0:k}) \pi_k(x_{0:k}) dx_{0:k} \quad (1)$$

where $x_{0:k}^{(i)} i=1...N$ is a set of support points, $w_k^{(i)}$ is the associated weight, $x_{0:k}$ corresponds to the state trajectory from time 0 to k and ϕ_k is any integrable function π_k. The target distribution is chosen as $\pi_k(x_{0:k}) = p(x_{0:k}|y_{1:k-1})$, which is the a posteriori pdf state vector, conditioned by the noisy observations $y_{1:k}$ [22]. As in any Bayesian process, the estimation process involves two main stages: prediction and update. In the prediction stage, the trajectories of the state vector are extended using a distribution of arbitrary importance $q(\tilde{x}_{0:k}|x_{1:k-1})$, where $\tilde{x}_{0:k_{(i)}} = (x_{0:k-1}, \tilde{x}_k)$. In the update stage, the new weights $w_k^{(i)}$ are evaluated by the measurement of probability using $w_k^{(i)} \propto w_{k-1}^{(i)} \cdot p(y_k|\tilde{x}_{0:k}) p(\tilde{x}|x_{0:k-1}) / q(\tilde{x}_{0:k}|x_{0:k-1})$, where $\sum_{i=1}^{N} w_k^{(i)} = 1$ [10].

The efficiency of this process is improved if the variance of the weights of the particles is minimized [22]. A common problem with the sequential importance sampling is the phenomenon of degeneration, where a few particles begin to have higher weights, while others appear with decreasing weights. The latter case requires a significant computational cost that is engaged in updating particles whose contribution to the a posteriori pdf is negligible. A technique to see if this phenomenon occurs, is to calculate the index:

$$N_{eff} = \frac{1}{\sum_{i=1}^{N} (w_k^i)^2} \quad (2)$$

where w_k^i is the normalized particle weight. N_{eff} is a value between 0 and N, where the degeneration is considered to occur when the value N_{eff} is less than $0.85N$ [27].

III. Implementation

To estimate the SOC based on PF it is required to have a state-space representation model. In this work, it is proposed to use the phenomenological empirical model presented in [10] and it is defined according to (3), (4), and (5), where $x_1(k)$ is an unknown parameter associated to internal impedance and it is estimated applying artificial evolution concept, x_2 is the measure of SOC; $i(k)$ and $v(k)$ are the current and voltage of the battery at time k; Δt is the sample time; E_{crit} is the expected total energy delivery by the battery; ω_1, ω_2 correspond to the noises of the process and n is the observation noise. The parameter v_0, v_l, γ, α and β are model parameters and they are estimated off-line. v_0 is the voltage when the battery is fully charged, v_l is the y-intercept of the extrapolation of the second zone and γ, α, β are parameters associated to the three zones in which the curve of the open circuit voltage (OCV) is divided.

State transition equations:

$$x_1(k+1) = x_1(k) + \omega_1(k) \quad (3)$$

$$x_2(k+1) = x_2(k) - v(k) * i(k) \Delta t \, E_{crit}^{-1} + \omega_2(k) \quad (4)$$

Measurement equation:

$$\begin{aligned} v(k) &= v_l + (v_o - v_l) e^{\gamma(x_2(k)-1)} +_l (x_2(k) - 1) \\ &+ (1-\alpha) v_l (e^{-\beta} - e^{-\beta\sqrt{x_2(k)}}) - i(k) * x_1 + n(k) \end{aligned} \quad (5)$$

In [10], the OCV curve is described for (6), where the V_{oc} is the open-circuit voltage, $v(k)$ is the voltage in the terminal battery in the time k, $i(k)$ is the current and Z_p is the internal impedance.

$$V_{oc} = v(k) + i(k) Z_p \quad (6)$$

From (6) we obtain the observation equation of the state space model, where V_{oc} is defined according three zone, see Figure (1). The first zone exhibits an exponential decay that covers the range of SOC > 0.70 and it is mainly dominated by the parameter γ (see (5)). The second zone covers the range between $0.25 <$ SOC ≤ 0.7. This region exhibits a

linear behavior and it is mainly influenced by the parameter α. Finally, the third zone, which resides in the remaining range of SOC ≤ 0.25, shows a sharp drop in voltage. This behavior is mainly associated to the effect of the parameter β.

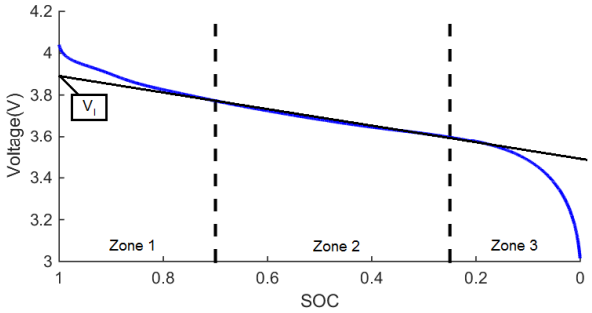

Fig. 1: Discharge open circuit voltage

To improve the decision-making process in the use of available energy in the battery, it is proposed to avoid that the battery voltage is in the third zone of OCV curve (abrupt voltage drop), that is to say $SOC < 0.25$. α is a parameter that allows to determine if the battery is about to enter the third zone of OCV curve, shown in Figure 6. As indicated previously, α is associated with the second region of the OCV curve and which accounts for longer battery operation. In this work, the SOC and α parameter are estimated to obtain information that prevents battery misuse.

The estimation of the parameter α implies making modifications to the original model, since the state x_1 is associated with the internal impedance of the battery. The state-space model used (with corresponding changes) is defined by (7), (8), and (9). For this model the state x_1 is associated to the α parameter, whereα is the variable that defines the linear zone of the OCV curve.

State transition equations:

$$\alpha(k+1) = \alpha(k) + \omega_1(k) \tag{7}$$

$$\begin{aligned} x_2(k+1) = x_2(k) - \Big(v_l + (v_o - v_l)e^{\gamma(x_2(k)-1)} \\ +\alpha(k)v_l(x_2(k)-1)+(1-\alpha(k))v_l(e^{-\beta}-e^{-\beta\sqrt{x_2(k)}}) \\ - i(k)Z_{int} + n(k)\Big) i(k)\Delta t\, E_{crit}^{-1} + \omega_2(k) \end{aligned} \tag{8}$$

Measurement equation:

$$\begin{aligned} v(k) = v_l + (v_o - v_l)e^{\gamma(x_2(k)-1)} + \alpha(k)v_l(x_2(k)-1) \\ + (1-\alpha(k))v_l(e^{-\beta} - e^{-\beta\sqrt{x_2(k)}}) - i(k)Z_{int} + n(k) \end{aligned} \tag{9}$$

Once the state-space representation model is defined, the electrical current and voltage data are required as input variables. The data acquisition is done through the complete discharge of a LIR2032 battery with a 45 mAh capacity and a 3.6 V nominal voltage. The battery discharge execution requires a consumption profile, which indicates the amount of electrical current demanded from battery by the system at specific scheduled instances. In this work, two profiles are deployed that mimic the energy consumption associated with the operating modes of the CC2500 transceiver. The execution cutoff voltage condition used is 3 V. The first power usage profile uses a constant 22-mA-current scenario. This gives us a baseline for a worse-case scenario where continuous transmissions occur. The second power usage profile uses a random generated sequence, with randomly generated intervals (up to 30 seconds) that has electrical currents alternating between two values: 14 mA and 22 mA. The current and voltage values obtained from the first set are used to determine the parameters offline (not in real-time) and to estimate the SOC by making adjustments to the PF algorithm, while the results obtained from the second profile execution are used for validation. In addition to the state-space representation model, the electrical current and voltage data is necessary to establish the filter parameters to estimate the SOC based on the PF. In this work, the parameters used will be set to 40 particles and 25 embodiments according to the terms of [28].

To validate the decision by the MAC protocol a simulated test is set up that includes the participation of four sensor nodes, where the transmission periods of each node are assigned randomly and the electrical current is only drawn from the battery during this operating mode. The algorithm is designed such that after a transmission the amount of available energy in the battery is estimated and no transmissions occur after the batteries of the sensors reach a SOC ≤ 0.25.

IV. Results

The discharge tests performed on the LIR2032 battery, using constant current and the random profile, allow to obtain the curves V_{oc} vs SOC curves shown in Figure 2.

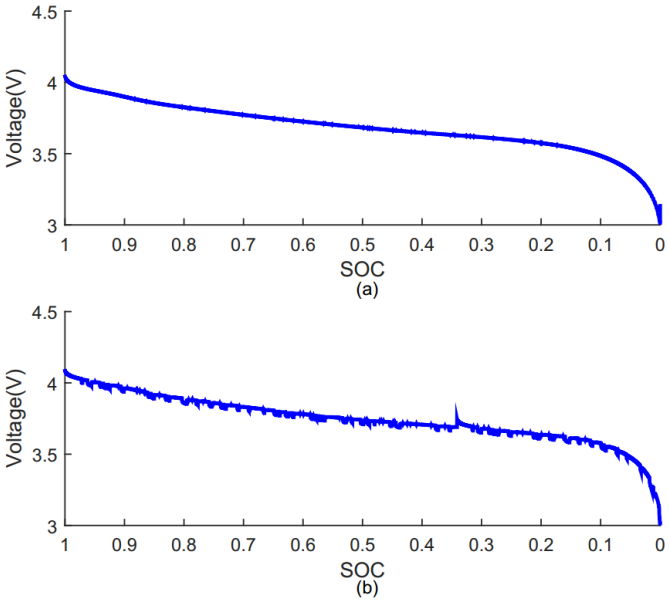

Fig. 2: Discharge open Circuit Voltage: (a) Constant Current (b) Random Profile

The curve V_{oc} vs SOC obtained from the constant current discharge allow to estimate the model parameters offline (not real-time), which are shown in Table I.

TABLE I: Model Parameters for Battery LIR2032

Battery	v_o	v_l	α	β	γ	E_{crit}
LIR2032	4.0402	3.881	0.09981	15.53	11.29	519

To estimate the SOC it is important to have adequate characterization of the regions 1 and 2 of the V_{oc} vs SOC curve, as those are the governing parameters that determine the battery behavior. Even though the third region is heavily influenced by the parameter β and, ideally, this region should be avoided, estimating the value of β is still beneficial to increase the accuracy of the model.

For the SOC estimation based on PF it is necessary to define the noises associated with the model. These parameters were calculated through the covariance matrix between the experimental and adjusted data, in addition to making empirical adjustments according to the PF performance. Determining all parameters of the model, the algorithm was initially executed using the current and voltage data obtained from the discharge to the battery at constant current (22mA). Time used for the estimation of α, voltage and SOC is 6448 seconds, which is the time it takes the battery to reach the cut condition. Figure 3 shows the results of the voltage and α estimation. In the Figure 4 we can see the precision in the SOC estimation.

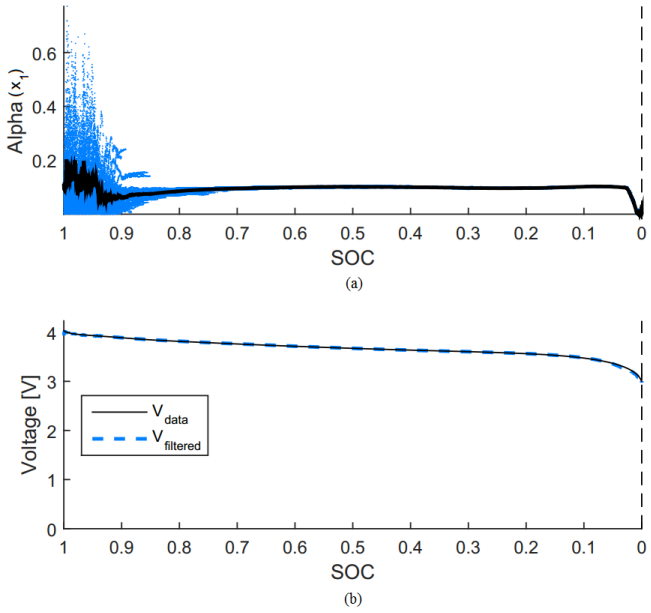

Fig. 3: (a) Evolution of the state x_1. (b) Measured Voltage and Estimated Voltage

To validate the correct operation of the filter, a second set of data generated from the random profile described in section 2 is used. The estimation of α, voltage and SOC are performed for a time of 9542 seconds, see Figure 5 and 6. The results obtained in Figures 3 and 5 show that for values of $SOC > 0.7$, the α parameter oscillates and that for $0.25 < Soc \leq 0.7$, α is able to remain constant. This behavior validates the theoretical concepts described in section 2. In Figures 4 and 6 we can see that the filter is capable of correcting errors in the initial condition of the SOC, for example in Figure 6 for $SOC > 70\%$, the filter performs an overestimation but subsequently adjusts and achieves a more accurate estimate.

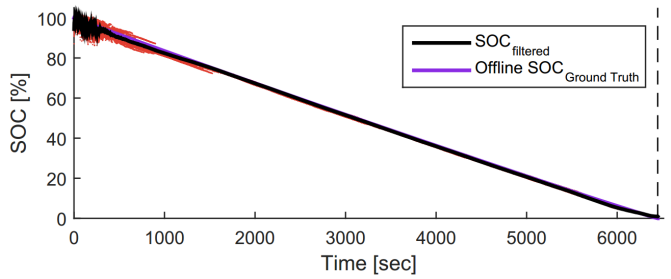

Fig. 4: SOC Estimation

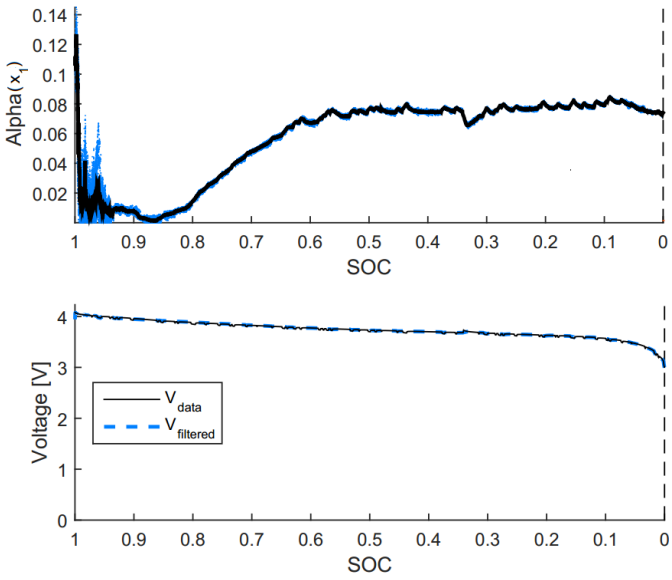

Fig. 5: (a) Evolution of the state x_1. (b) Measured Voltage and Estimated Voltage

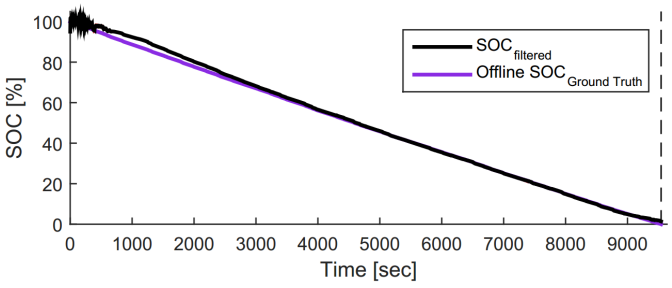

Fig. 6: SOC Estimation

The results obtained in the estimation of the parameter α confirm that this parameter can be used as an indicator, since

for values of $0.25 < Soc \leq 0.7$ the filter can maintain a constant behavior, which would allow us to establish that some abrupt change in the value of α would indicate low energy availability in the battery.

From the data obtained from the estimation of the alpha parameter and the SOC, a series of simulated tests were performed to emulate decision making by the MAC protocol. The results obtained are shown in Figure 7, which clearly shows that the sensor node 2 reached the cutting condition SOC ≤ 0.25, hence, it is necessary to cease transmission. Moreover, the feedback from these results enables the system to establish a transmission order according to the amount of energy available in each sensor. For example, sensor node 4 has 58% of the total energy capacity, while the sensor node 3 only has 27% of its energy remaining.

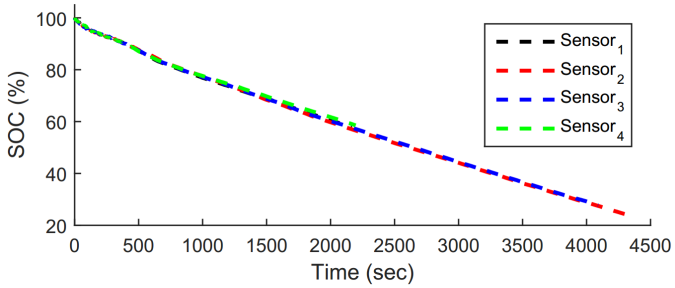

Fig. 7: Amount of energy available in each Sensor

Another advantage that is emphasized is that useful information can be delivered to the MAC protocol (shown in Figure 8), where it can be observed that the sensor-node-3 battery must temporarily enter a charging mode, while sensor nodes 1 and 4 are prioritized for transmission as these still have energy (have not reached the cutting condition).

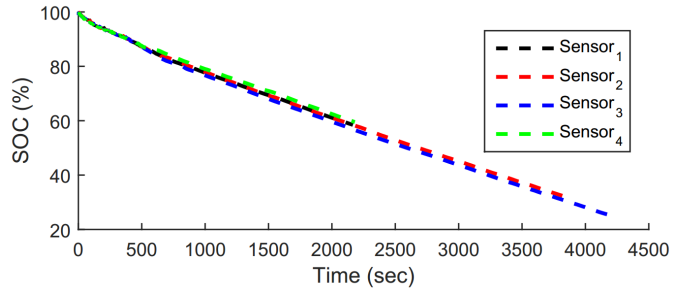

Fig. 8: Amount of energy available in each Sensor

V. Conclusion

This work presents the SOC estimation based on the PF for batteries used in the sensor nodes of WSNs. The proposed mechanisms generate useful information to MAC protocols that allows it to improve the energy efficiency of the network as well as extend the life of the batteries, by preventing these from fully discharging. From the data obtained, two battery power consumption profiles are studied and compared taking two criteria in account: first, a continuous battery usage which gives us a baseline to establish the worst-case scenario where the sensor node continuously transmits (drawing constant current), therefore discharging at the quickest rate possible. The second profile is generated to establish a usage that is representative of expected transitions between the operating modes of the sensor node. Through the simulated tests it is found that the PF is able to adjust and deliver accurate and useful SOC estimations. Despite the implications of using particle-filter algorithms, such as computational overhead, the benefits in terms of real-time estimation accuracy justify its implementation in battery-SOC estimation applications.

Acknowledgment

This work was partially supported by the Universidad Tecnológica de Panama, IFARHU (Grant for Doctoral Studies), and CONICYT-PCHA/Doctorado Nacional/2016-21161427.

References

[1] C. Estevez, M. Orchard, and A. Kailas, "Improving throughput performance under an energy efficient multiplexing access scheme using time-of-failure prognosis," in *Proceedings of the 8th International Conference on Body Area Networks*. ICST (Institute for Computer Sciences, Social-Informatics and Telecommunications Engineering), 2013, pp. 390–393.

[2] T. R. Rao, D. Balachander, N. Tiwari, and P. Mvsn, "Ultra-high frequency near-ground short-range propagation measurements in forest and plantation environments for wireless sensor networks," *IET Wireless Sensor Systems*, vol. 3, no. 1, pp. 80–84, 2013.

[3] J. Ko, C. Lu, M. B. Srivastava, J. A. Stankovic, A. Terzis, and M. Welsh, "Wireless sensor networks for healthcare," *Proceedings of the IEEE*, vol. 98, no. 11, pp. 1947–1960, 2010.

[4] C. Estevez and C. Azurdia, "Bottom-layer solutions for 60 ghz millimeter-wave wireless networks: modulation and multiplexing access techniques," *Telecommunication Systems*, vol. 61, no. 4, pp. 755–771, 2016.

[5] P. Huang, L. Xiao, S. Soltani, M. W. Mutka, and N. Xi, "The evolution of mac protocols in wireless sensor networks: A survey," *IEEE Communications Surveys & Tutorials*, vol. 15, no. 1, pp. 101–120, 2013.

[6] J. Zheng and A. Jamalipour, *Wireless sensor networks: a networking perspective*. John Wiley & Sons, 2009.

[7] P. Pal and P. Chatterjee, "A survey on tdma-based mac protocols for wireless sensor network," *International Journal of Emerging Technology and Advanced Engineering*, vol. 4, no. 6, pp. 219–230, 2014.

[8] K. Biswas, V. Muthukkumarasamy, X.-W. Wu, and K. Singh, "An analytical model for lifetime estimation of wireless sensor networks," *IEEE Communications Letters*, vol. 19, no. 9, pp. 1584–1587, 2015.

[9] R. J. Lajara, J. J. Perez-Solano, and J. Pelegri-Sebastia, "A method for modeling the battery state of charge in wireless sensor networks," *IEEE Sensors Journal*, vol. 15, no. 2, pp. 1186–1197, 2015.

[10] D. A. Pola, H. F. Navarrete, M. E. Orchard, R. S. Rabié, M. A. Cerda, B. E. Olivares, J. F. Silva, P. A. Espinoza, and A. Pérez, "Particle-filtering-based discharge time prognosis for lithium-ion batteries with a statistical characterization of use profiles," *IEEE Transactions on Reliability*, vol. 64, no. 2, pp. 710–720, 2015.

[11] M. E. Orchard, P. Hevia-Koch, B. Zhang, and L. Tang, "Risk measures for particle-filtering-based state-of-charge prognosis in lithium-ion batteries," *IEEE Transactions on Industrial Electronics*, vol. 60, no. 11, pp. 5260–5269, 2013.

[12] W. Rukpakavong, L. Guan, and I. Phillips, "Dynamic node lifetime estimation for wireless sensor networks," *IEEE Sensors Journal*, vol. 14, no. 5, pp. 1370–1379, 2014.

[13] L. B. Hörmann, P. M. Glatz, C. Steger, and R. Weiss, "Measuring the state-of-chargeanalysis and impact on wireless sensor networks," in *Local Computer Networks (LCN), 2011 IEEE 36th Conference on*. IEEE, 2011, pp. 982–985.

[14] K. S. Ng, C.-S. Moo, Y.-P. Chen, and Y.-C. Hsieh, "Enhanced coulomb counting method for estimating state-of-charge and state-of-health of lithium-ion batteries," *Applied energy*, vol. 86, no. 9, pp. 1506–1511, 2009.

[15] I. Snihir, W. Rey, E. Verbitskiy, A. Belfadhel-Ayeb, and P. H. Notten, "Battery open-circuit voltage estimation by a method of statistical analysis," *Journal of Power Sources*, vol. 159, no. 2, pp. 1484–1487, 2006.

[16] L. Ran, W. Junfeng, W. Haiying, and L. Gechen, "Prediction of state of charge of lithium-ion rechargeable battery with electrochemical impedance spectroscopy theory," in *Industrial Electronics and Applications (ICIEA), 2010 the 5th IEEE Conference on*. IEEE, 2010, pp. 684–688.

[17] A. J. Salkind, C. Fennie, P. Singh, T. Atwater, and D. E. Reisner, "Determination of state-of-charge and state-of-health of batteries by fuzzy logic methodology," *Journal of Power Sources*, vol. 80, no. 1, pp. 293–300, 1999.

[18] M. Charkhgard and M. Farrokhi, "State-of-charge estimation for lithium-ion batteries using neural networks and ekf," *IEEE transactions on industrial electronics*, vol. 57, no. 12, pp. 4178–4187, 2010.

[19] W. Wang, H. S.-H. Chung, and J. Zhang, "Near-real-time parameter estimation of an electrical battery model with multiple time constants and soc-dependent capacitance," *IEEE Transactions on Power Electronics*, vol. 29, no. 11, pp. 5905–5920, 2014.

[20] R. Ahmed, M. El Sayed, I. Arasaratnam, J. Tjong, and S. Habibi, "Reduced-order electrochemical model parameters identification and state of charge estimation for healthy and aged li-ion batteriespart ii: Aged battery model and state of charge estimation," *IEEE Journal of Emerging and Selected Topics in Power Electronics*, vol. 2, no. 3, pp. 678–690, 2014.

[21] G. Welch and G. Bishop, "An introduction to the kalman filter. department of computer science, university of north carolina," 2006.

[22] M. E. Orchard and G. J. Vachtsevanos, "A particle-filtering approach for on-line fault diagnosis and failure prognosis," *Transactions of the Institute of Measurement and Control*, 2009.

[23] M. Berecibar, I. Gandiaga, I. Villarreal, N. Omar, J. Van Mierlo, and P. Van den Bossche, "Critical review of state of health estimation methods of li-ion batteries for real applications," *Renewable and Sustainable Energy Reviews*, vol. 56, pp. 572–587, 2016.

[24] M. Mastali, J. Vazquez-Arenas, R. Fraser, M. Fowler, S. Afshar, and M. Stevens, "Battery state of the charge estimation using kalman filtering," *Journal of Power Sources*, vol. 239, pp. 294–307, 2013.

[25] D. Antolín, N. Medrano, and B. Calvo, "Reliable lifespan evaluation of a remote environment monitoring system based on wireless sensor networks and global system for mobile communications," *Journal of Sensors*, vol. 2016, 2016.

[26] D. Jiani, W. Youyi, and W. Changyun, "Li-ion battery soc estimation using particle filter based on an equivalent circuit model," in *2013 10th IEEE International Conference on Control and Automation (ICCA)*. IEEE, 2013, pp. 580–585.

[27] M. S. Arulampalam, S. Maskell, N. Gordon, and T. Clapp, "A tutorial on particle filters for online nonlinear/non-gaussian bayesian tracking," *IEEE Transactions on signal processing*, vol. 50, no. 2, pp. 174–188, 2002.

[28] B. E. Olivares, M. A. C. Munoz, M. E. Orchard, and J. F. Silva, "Particle-filtering-based prognosis framework for energy storage devices with a statistical characterization of state-of-health regeneration phenomena," *IEEE Transactions on Instrumentation and Measurement*, vol. 62, no. 2, pp. 364–376, Feb 2013.